iScience, Volume *23*

Supplemental Information

The Cytokine Receptor IL-7Rα Impairs IL-2 Receptor Signaling and Constrains the *In Vitro* Differentiation of Foxp3^{+} Treg Cells

Adam T. Waickman, Hilary R. Keller, Tae-Hyoun Kim, Megan A. Luckey, Xuguang Tai, Changwan Hong, Carmen Molina-París, Scott T.R. Walsh, and Jung-Hyun Park

Supplemental Figure S1

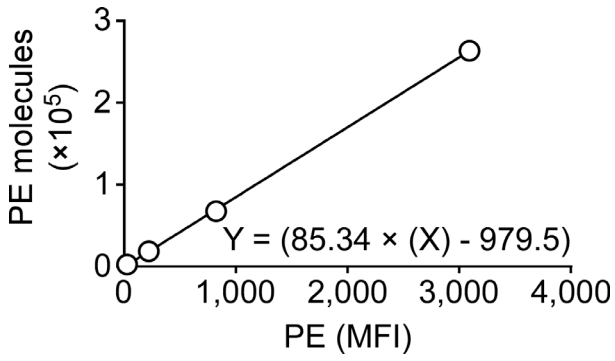

Figure S1. Methodology for receptor number quantification. Related to Figure 1.
PE-conjugated calibration beads (BANG laboratories) were analyzed by flow cytometry at the same time as live cells stained with saturating concentrations of PE-conjugated antibodies against cytokine receptors of interest. Linear regression calculation was performed using the corrected Mean Fluorescence Intensity (MFI) values from the PE calibration beads and known number of PE molecules per bead. The resulting equation was used to calculate the number of cytokine receptors present on live cells, using the corrected PE MFI values from each cytokine receptor analyzed.

Supplemental Figure S2

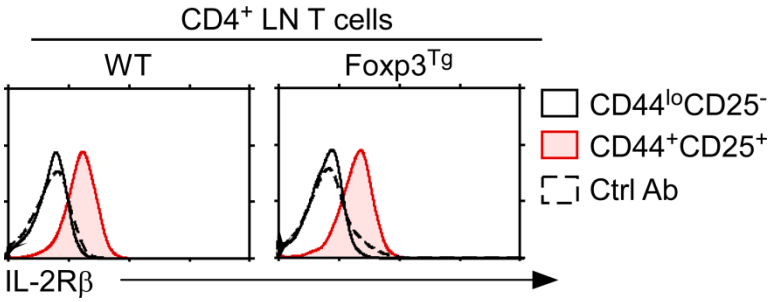

Figure S2. IL-2Rβ expression on Foxp3^{Tg} CD4^{+} LN T cells. Related to Figure 2.
Surface IL-2Rβ expression was assessed on naive (CD44^{lo}CD25^{-}) and activated/memory phenotype (CD44^{hi}CD25^{+}) CD4^{+} LN T cells from WT and Foxp3^{Tg} mice. Results are representative of 2 independent experiments.

Supplemental Figure S3

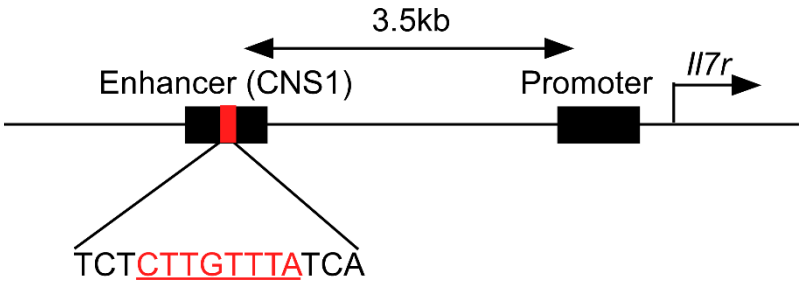

Figure S3. Putative Foxp3 binding site in the putative *Il7r* enhancer (CNS1). Related to Figure 2. Evolutionally-conserved promoter and putative enhancer (CNS1) regions of the *Il7r* gene locus were identified using the rVISTA software. A conserved Foxp3-binding site was identified in the enhancer region. However, the same analysis failed to identify a Foxp3-binding site in the promoter region.

Supplemental Figure S4

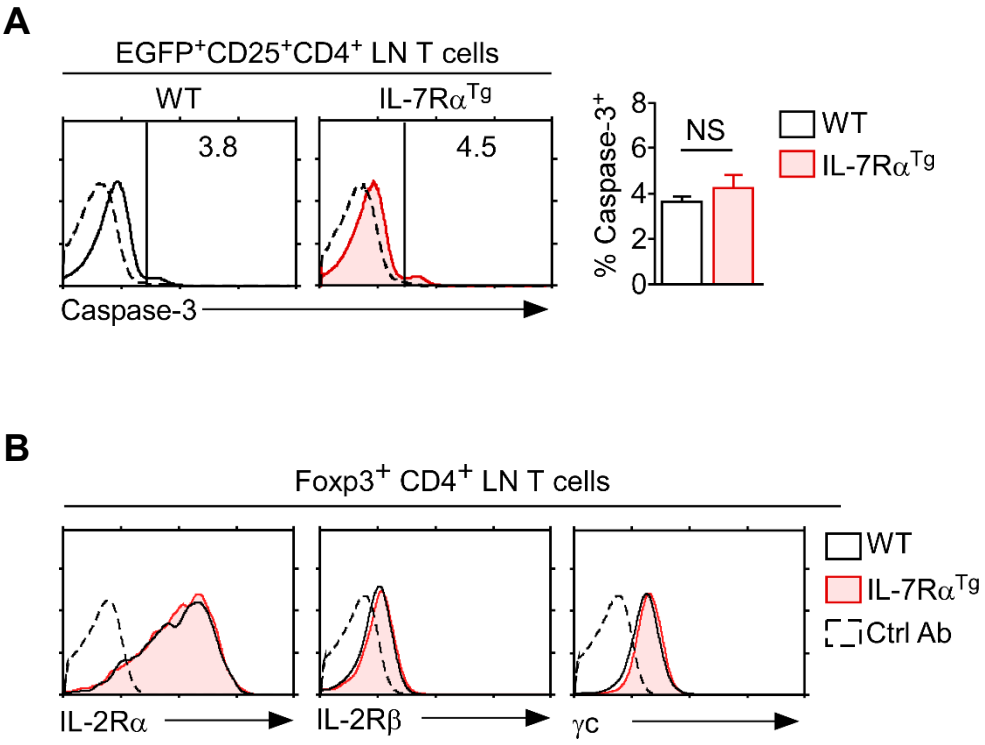

Figure S4. Phenotypic analysis of IL-7Rα^{Tg} Foxp3^{+} Treg cells. Related to Figure 3.
(A) Caspase-3 activity was assessed in Foxp3-EGFP reporter mice that were either WT or additionally transgenic for IL-7Rα (IL-7Rα^{Tg}). Active caspase-3 was visualized using CaspGLOW Red Caspase-3 substrates followed by flow cytometry. Histograms are representative and bar graphs are summary of two independent experiments, showing mean wth SEM.
(B) Expression of the high-affinity IL-2 receptor subunits, IL-2Rα, IL-2Rβ and γc, on Foxp3^{+} CD4^{+} LN T cells of WT and IL-7Rα^{Tg} mice. Histograms are representative of 2 independent experiments. Unpaired two-tailed Student's t-test, where *P<0.05, **P<0.01, *** P<0.001, **** P<0.0001.

Supplemental Figure S5

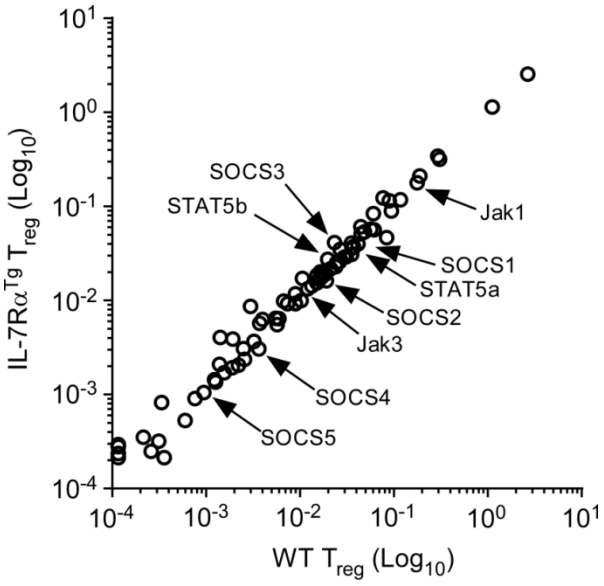

Figure S5. JAK/STAT pathway analysis of WT and IL-7Rα^{Tg} Treg cells. Related to Figure 3. RNA was isolated from electronically sorted CD4^{+}CD25^{+} T cells (Tregs) of WT and IL-7Rα^{Tg} mice. Relative mRNA expression of molecules in the JAK/STAT signaling pathway was assessed using the QIAgen RT^{2} Profiler PCR array. Key genes involved in IL-2 and IL-7 receptor signaling are indicated.

Supplemental Figure S6

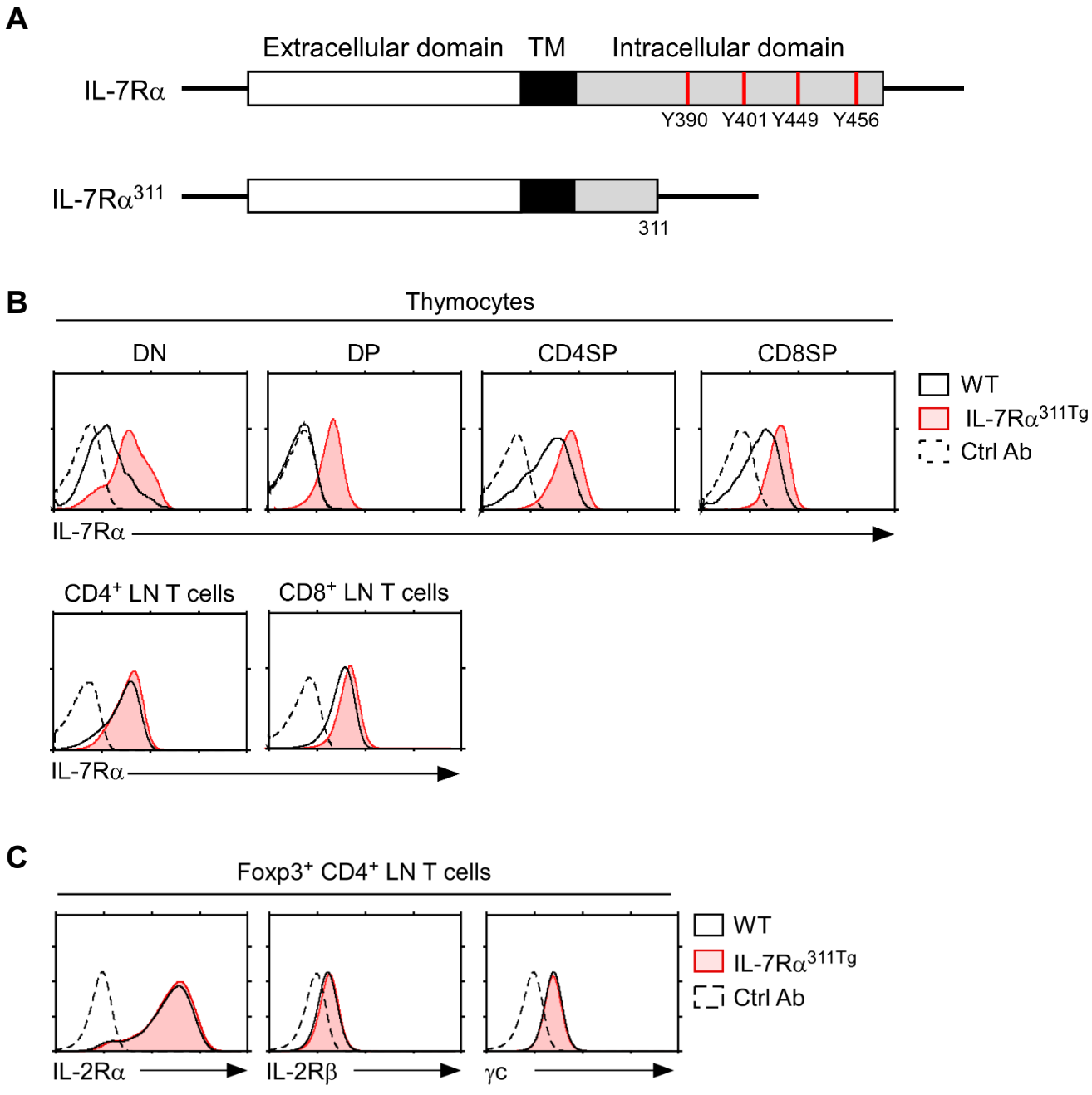

Figure S6. Cytokine receptor expression on IL-7Rα^{311Tg} T cells. Related to Figure 5.
(A) The IL-7Rα consists of an extracellular (239 a.a.), transmembrane (25 a.a.), and intracellular (195 a.a.) protein domain. The IL-7Rα^{311} is a truncated form of the full-length IL-7Rα and lacks the membrane-distal 148 amino acids, thus eliminating all four tyrosine residues and disabling IL-7 receptor signaling.
(B) Surface IL-7Rα expression on thymocytes (top) and LN T cells (bottom) of WT and IL-7Rα^{311Tg} mice. Histograms are representative of 2 independent experiments.
(C) Expression of the high-affinity IL-2 receptor subunits, IL-2Rα, IL-2Rβ and γc, on Foxp3^{+} CD4^{+} LN T cells of WT and IL-7Rα^{311Tg} mice. Histograms are representative of 2 independent experiments.

Supplemental Figure S7

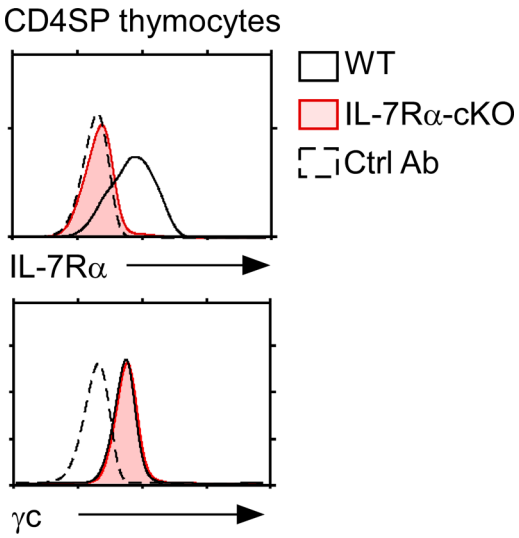

Figure S7. Cytokine receptor expression on IL-7Rα-cKO CD4SP thymocytes. Related to Figure 6.
Cell surface staining for IL-7Rα and γc on WT and IL-7Rα-cKO CD4SP thymocytes. Results are representative of three independent experiments.

Transparent Methods

Mice

C57BL/6 (B6) and Ly5.2 congenic mice of both sexes were purchased from Charles River Laboratories and used for analysis between 6 – 20 weeks of age. Foxp3^{Tg}, IL-7Rα^{Tg}, IL-7Rα^{KO}, IL-7Rα-cKO and Foxp3-EGFP reporter mice have been previously described (Tai et al., 2013, Peschon et al., 1994, Yu et al., 2006, Zhou et al., 2008). The IL-7Rα-conditional KO mice were previously reported and were kindly provided by A. Singer (National Cancer Institute, National Institutes of Health, Bethesda, MD) (McCaughtry et al., 2012). The IL-7Rα-GFP reporter mice express an IRES-GFP BAC transgene that is inserted into the 5'-UTR of the *Il7r* gene locus. GFP levels in cells isolated from this mouse faithfully indicate the level of IL-7Rα gene transcription (Ligons et al., 2012). IL-7Rα^{311Tg} transgenic mice were produced by generating a truncated IL-7Rα cDNA construct lacking all C-terminal residues downwards of a.a. 312 of the mouse IL-7Rα cytosolic tail. This cDNA construct was cloned into a human *CD2* enhancer-promoter-based vector and injected into fertilized B6 oocytes to generate IL-7Rα^{311Tg} mice (**Figure S7**). For all animal experiments, we routinely analyzed mice of both sexes that were aged between 6 -20 weeks. Animal experiments were approved by the NCI Animal Care and Use Committee, and all mice were cared for in accordance with NIH guidelines. All experiments conform to the regulatory standards of the NIH.

Surface plasmon resonance (SPR) analysis

Purified murine IL-7Rα and IL-2Rβ ECDs expressed from human or yeast cells were purchased from Sino Biological, Inc. (Wayne, PA), and LifeSpan Biosciences, Inc. (Seattle, WA), respectively. Purified murine γc ECD with a C-terminal Fc fusion expressed from Sf21 insect cells was purchased from R&D Systems, Inc. (Minneapolis, MN). Finally, murine IL-7Rα ECD was also expressed and purified from S2 insect cells using similar procedures described previously by the Walsh laboratory (Wickham and Walsh, 2007). Protein concentrations were determined from amino acid composition of the number of Tyr and Trp residues (Pace et al., 1995). All proteins were exchanged into HBS-EP buffer (10 mM HEPES, pH 7.4; 150 mM NaCl; 3 mM EDTA; and 0.005% Tween-20) using NAP-5 (GE) desalting columns. The γc ECD-

Fc fusion was amine-coupled to a CM5 sensor chip using similar methods as those described previously (Hong et al., 2014). For the IL-2Rβ/γc interaction, a concentration series of IL-2Rβ was injected over immobilized γc at a flow rate of 25 μl/min in HBS-EP (pH 7.4) buffer. SPR sensorgrams were double referenced and trimmed using BIAevaluation 4.1 software (GE). Dose-response curves (R_{max} *vs* [IL-2Rβ]) were generated and fit using Prism 5.0 (GraphPad) to determine the K_d values. For the IL-7Rα/γc interaction, a concentration series of IL-7Rα was injected over immobilized γc at a flow rate of 50 μl/min. These sensorgrams were double referenced, trimmed, and globally fit using Clamp XP to determine the binding constants (k_{on}, k_{off}. and $K_d = k_{off}/k_{on}$). SPR experiments were performed 3-4 times at 25 °C using a Biacore 3000 instrument (GE), the values were averaged, and propagated errors were estimated.

Flow cytometry

Cells were analyzed using FACSCalibur, FACSAria, or LSR II cell sorters (BD Biosciences; San Jose, CA) and software designed by the Division of Computer Research and Technology at the NIH. The cells were gated using the forward scatter exclusion of dead cells stained with propidium iodide. For nuclear staining, the cells were first surface stained, fixed, and then permeabilized using a Foxp3 intracellular staining kit, according to the manufacturer's instructions (Thermo Fisher eBioscience; Waltham, MA). The cells were surface stained with antibodies against IL-7Rα (A7R34, eBioscience), IL-2Rβ (TMβ1, BD Biosciences), γc (4G3, BD Biosciences), IL-4Rα (mIL4R-M1, BD Biosciences), IL-21R (4A9, BioLegend; San Diego, CA), TCRβ (H57-597, BD Biosciences), CD4 (GK1.5, BioLegend), CD8α (C53-6.7, BioLegend), and CD45.1 (A20, BioLegend).

Receptor abundance calculation

T cell cytokine receptor abundance was calculated as previously described (Cotari et al., 2013, Gonnord et al., 2018). Briefly, LN T cells from WT or Foxp3-EGFP reporter mice were stained with a saturating concentration (as determined by titration) of PE-conjugated anti-γc, anti-IL-7Rα, anti-IL-2Rβ, or isotype control antibodies and analyzed by flow cytometry. The corrected mean fluorescent intensity (MFI) for PE was calculated by subtracting the MFI of the isotype control antibody from the MFI of the individual

antibodies. A standard curve correlating the PE MFI values to a known number of PE molecules was generated using Quantum R-PE MESF beads (Bangs Laboratories; Fishers, IN) analyzed by flow cytometry. The corrected MFI for the Quantum R-PE MESF beads was calculated by subtracting the MFI of the unlabeled beads from the MFI of the beads with a known number of PE molecules (**Figure S1**). This standard curve was used to calculate the number of receptors on the surface of the stained T cells using a ratio of one PE molecule per antibody, as specified by the manufacturer (eBioscience or BD Bioscience)

Intracellular staining for pSTAT5 and Foxp3

Following cytokine stimulation, LN T cells were fixed using a Foxp3 intracellular staining kit (eBioscience) at 4°C. Cells were washed with permeabilization buffer (eBioscience) and stained with Alexa Fluor-647-conjugated anti-Foxp3 antibodies (FJK-16, eBioscience) for 30 min at room temperature. Cells were washed, re-fixed using 2% paraformaldehyde at 4°C, and permeabilized using 90% methanol. The cells were then stained with anti-pSTAT5 (47, BD Biosciences) at room temperature for 30 min, followed by staining with anti-CD4 (GK1.5, Tonbo Biosciences; San Diego, CA) and anti-CD25 (PC61.5, eBioscience).

Active caspase-3 staining

LN cells from Foxp3-GFP and IL-7Rα^{Tg} Foxp3-GFP mice were incubated overnight at 37°C in medium, washed, and then incubated for 45 min with CaspGLOW Red caspase-3 substrate (BioVision; Milpitas, CA). Dead cells were excluded by staining with reagents from a LIVE/DEAD Fixable Aqua Dead Cell Stain kit (Thermo Fisher), and cells were analyzed by flow cytometry.

RT-PCR array

Total RNA was isolated from sorted cells using an RNAeasy micro kit (Qiagen; Germantown, MD). cDNA was generated using oligo(dT) primers and the QuantiTect reverse transcription kit (Qiagen). Quantitative RT-PCR was performed using an ABI PRISM 7900HT system and QuantiTect SYBR Green (Qiagen).

***In vitro* Foxp3$^+$ regulatory T cell differentiation**

Naïve LN CD4$^+$ T cells were enriched by negative magnetic selection (StemCell; Cambridge, MA), and their purity was confirmed by flow cytometry. Enriched cells were stimulated with 1 μg/ml plate bound anti-CD3/CD28 for 4 days in the presence of 5 ng/ml TGF-β and increasing amounts (0-10 ng/ml) of IL-2 or IL-7 (PeproTech; Rocky Hill, NJ). After differentiation, the cells were counted, and the expression of intracellular Foxp3 proteins was determined by flow cytometry.

***In vitro* Th17 T cell differentiation**

Naïve LN CD4$^+$ T cells from WT, IL-7Rα^{Tg}, or IL-7Rα-cKO mice were enriched by negative magnetic selection (StemCell), and purity was confirmed by flow cytometry. Mature CD4SP CD44^{lo} thymocytes were electronically sorted. The cells were stimulated with 1 μg/ml plate bound anti-CD3/CD28 for 5 days in the presence of 5 ng/ml TGF-β, 10 ng/ml IL-6 (PeproTech), anti-IFN-γ (R4-6A4, BioLegend) and anti-IL-4 (11B11, BioLegend).

Survival assay of adoptively transferred Foxp3$^+$ Treg cells

CD4$^+$ T cells were enriched by depleting CD8$^+$ T cells and B cells from CD45.2$^+$ IL-7Rα^{Tg} Foxp3-GFP and congenic CD45.1$^+$ Foxp3-GFP LN cells with BioMag beads (Qiagen). The purified CD4$^+$ T cells from CD45.1$^+$ and CD45.2$^+$-origin mice were mixed at a 1:1 ratio before adoptive transfer into Rag2^{KO}IL-7^{KO}host mice. After 2 weeks of transfer, at day 14, the donor T cells were recovered from host LNs and assessed for the frequencies of CD45.1$^+$ and CD45.2$^+$ Foxp3-GFP$^+$ CD4 T cells. IL-7Rα^{Tg} Foxp3$^+$ versus WT Foxp3$^+$ CD4$^+$ T cell ratios among donor T cells were then compared to those before injection, at day 0.

Statistical analysis

Statistical differences of the mean with standard error of the mean (SEM) were analyzed by unpaired two-tailed Student's *t*-test or with 2-way ANOVA. *P* values of less than 0.05 were considered significant: **P*<0.05, ***P*<0.01, *** *P*<0.001, **** *P*<0.0001. All statistical analyses were performed using GraphPad Prism 6.

Supplemental References

Cotari, J. W., Voisinne, G., Dar, O. E., Karabacak, V. & Altan-Bonnet, G. 2013. Cell-to-cell variability analysis dissects the plasticity of signaling of common gamma chain cytokines in T cells. *Sci Signal,* 6**,** ra17.

Gonnord, P., Angermann, B. R., Sadtler, K., Gombos, E., Chappert, P., Meier-Schellersheim, M. & Varma, R. 2018. A hierarchy of affinities between cytokine receptors and the common gamma chain leads to pathway cross-talk. *Sci Signal,* 11.

Hong, C., Luckey, M. A., Ligons, D. L., Waickman, A. T., Park, J. Y., Kim, G. Y., Keller, H. R., Etzensperger, R., Tai, X., Lazarevic, V., Feigenbaum, L., Catalfamo, M., Walsh, S. T. & Park, J. H. 2014. Activated T cells secrete an alternatively spliced form of common gamma-chain that inhibits cytokine signaling and exacerbates inflammation. *Immunity,* 40**,** 910-23.

Ligons, D. L., Tuncer, C., Linowes, B. A., Akcay, I. M., Kurtulus, S., Deniz, E., Atasever Arslan, B., Cevik, S. I., Keller, H. R., Luckey, M. A., Feigenbaum, L., Moroy, T., Ersahin, T., Atalay, R., Erman, B. & Park, J. H. 2012. CD8 lineage-specific regulation of interleukin-7 receptor expression by the transcriptional repressor Gfi1. *J Biol Chem,* 287**,** 34386-99.

Mccaughtry, T. M., Etzensperger, R., Alag, A., Tai, X., Kurtulus, S., Park, J. H., Grinberg, A., Love, P., Feigenbaum, L., Erman, B. & Singer, A. 2012. Conditional deletion of cytokine receptor chains reveals that IL-7 and IL-15 specify CD8 cytotoxic lineage fate in the thymus. *J Exp Med,* 209**,** 2263-76.

Pace, C. N., Vajdos, F., Fee, L., Grimsley, G. & Gray, T. 1995. How to measure and predict the molar absorption coefficient of a protein. *Protein Sci,* 4**,** 2411-23.

Peschon, J. J., Morrissey, P. J., Grabstein, K. H., Ramsdell, F. J., Maraskovsky, E., Gliniak, B. C., Park, L. S., Ziegler, S. F., Williams, D. E., Ware, C. B., Meyer, J. D. & Davison, B. L. 1994. Early lymphocyte expansion is severely impaired in interleukin 7 receptor-deficient mice. *J Exp Med,* 180**,** 1955-60.

Tai, X., Erman, B., Alag, A., Mu, J., Kimura, M., Katz, G., Guinter, T., Mccaughtry, T., Etzensperger, R., Feigenbaum, L., Singer, D. S. & Singer, A. 2013. Foxp3 transcription factor is proapoptotic and lethal to developing regulatory T cells unless counterbalanced by cytokine survival signals. *Immunity,* 38**,** 1116-28.

Wickham, J., Jr. & Walsh, S. T. 2007. Crystallization and preliminary X-ray diffraction of human interleukin-7 bound to unglycosylated and glycosylated forms of its alpha-receptor. *Acta Crystallogr Sect F Struct Biol Cryst Commun,* 63**,** 865-9.

Yu, Q., Park, J. H., Doan, L. L., Erman, B., Feigenbaum, L. & Singer, A. 2006. Cytokine signal transduction is suppressed in preselection double-positive thymocytes and restored by positive selection. *J Exp Med,* 203**,** 165-75.

Zhou, X., Jeker, L. T., Fife, B. T., Zhu, S., Anderson, M. S., Mcmanus, M. T. & Bluestone, J. A. 2008. Selective miRNA disruption in T reg cells leads to uncontrolled autoimmunity. *J Exp Med,* 205**,** 1983-91.